

Modeling and Effective Foot Force Distribution for the Legs of a Quadruped Robot

Priyaranjan Biswal*  and Prases K. Mohanty 

*Department of Mechanical Engineering, National Institute of Technology, Arunachal Pradesh
791112, India*

E-mail: prases@nitap.ac.in

(Accepted December 4, 2020. First published online: January 8, 2021)

SUMMARY

This paper presents the detailed dynamic modeling of a quadruped robot. The forward and inverse kinematic analysis of each leg of the proposed model is deduced using Denavit-Hartenberg (D-H) parameters. It desires to calculate the optimal feet forces of the quadruped robot's joint torque, which is essential for its online control. To find out the optimal feet force distribution, two approaches are implemented to fulfill the locomotion objective. The four-legged quadruped robot and torso body's detailed dynamics are modeled to generate an equation of motion for the robot control system. The Euler-Lagrange theory has been used to find out the joint motion. The computer simulation results are presented to verify the effectiveness of the dynamic model.

KEYWORDS: Quadruped robot; Kinematics; Dynamics; Feet force; Power.

1. Introduction

In the last three decades, the mobile robot has made much attention because of exploring the complex environment, space, rescue operation, and accomplishing a task without human effort. The development of terrestrial locomotion of the legged robot has been continuously grown over the few decades because of more advantages than other robot vehicles.¹⁻³ The benefits of legged locomotion depend on the postures, the number of legs, and the functionality of the leg.⁴⁻⁶ A quadruped robot consists of many interconnecting parts, which leads to a complex issue in applied mechanics and robotics systems. Many problems bring into relation with each other like kinematics, gait planning, trajectory generation, and dynamics are to be solved for model-based control of quadruped robots. Because of such multibody systems complexity, it is essential to have a good mathematical model of kinematics and dynamics behaviors. In this context, Ding and Chen⁷ obtained dynamic modeling and locomotion control for quadruped robots based on the center of inertia. Gehring et al.⁸ developed a dynamic control gait for a quadruped robot. It is generally believed that Central Pattern Generators (CPG) are capable of producing rhythmic movements. A CPG network can coordinate all joints to complete a movement. Zhang et al. proposed the CPG model to achieve robust and dynamic trot gait, which can change its walking frequency online as well.⁹ Lin and Song proposed a kinematic and dynamic model of a quadruped model¹⁰ to analyze the stable locomotion and energy optimization during walking.

The contact points play a significant role in providing vital forces to keep the dynamic balance under external wrenches' influence made up of the inertial wrenches (force and moment) of moving links and gravity forces.¹¹⁻¹² Hence, force control is used for the effective assignment of trunk body force to the feet. At any instant point, the robot's three feet must be inside the support polygon

* Corresponding author. E-mail: priyaranjan.phd@nitap.ac.in

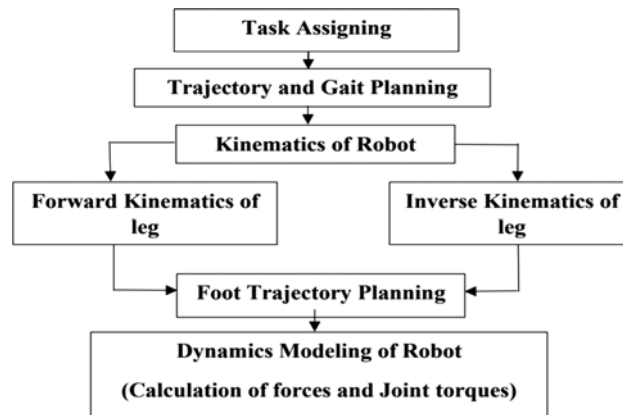


Fig. 1. Steps followed to implement the methodology.

to achieve a statically stable gait. During robot walking, the distribution of foot forces problem becomes indeterminate due to the closed-loop system.^{13,14} The force–moment equilibrium equation can be used to find multiple solutions where each tip of the foot is acted by a three-dimensional reaction force.^{15–18}

Chen et al.¹⁹ presented a new method for an optimal force distribution to estimate feet forces generated during ground contact by transforming the friction constraints. The method is characterized by shifting nonlinear inequalities into both linear equalities and linear inequalities. Zhou et al.²⁰ proposed a friction constraint method that is more practical-oriented than the pseudoinverse method.²¹ Moreover, the previous works, Marhefka and Orin,²² Zheng et al.,²³ Kar et al.²⁴ did not study a detailed model-based kinematic and locomotion performance objectives of the robot. However, the quadratic programming is used to calculate the feet force distribution in the six-legged robot that optimizes the energy exhaustion in the DC motor.²⁴ Hence, due to the inherent structural complexity of the multibody system like a walking robot, it is very tedious to incorporate inertial terms in the modeling.

In the majority of cases, simplified models of the robot are analyzed with kinematic and dynamic uncertainties. However, to better understand stable locomotion, such as dynamic stability and online control, a model-based realistic four-footed robot is necessary. In this paper, an investigation has been carried out on kinematics, dynamics, optimal feet force distribution, and its control of a realistic multi-legged robot.

2. Description of the Quadruped Robot and Modeling Methodology

A realistic CAD model of the four-legged robot is developed in Solidworks 2019 ×64 for study in this work. The main robot body consists of a rectangular torso with four identical legs. Each leg has three links connected by three actuators positioned in succession with symmetrically aligned with the torso's adjacent side. In mathematical modeling of the quadruped robot, the main objective is to find kinematics equations of all interconnected links and determine the desired joint variables to obtain the locomotion. Dynamic equations are also obtained for various uses like online control of robot motion, forces, trajectory design, and optimization. The sequence of steps computed to carry out the preferred methodology is shown in Fig. 1.

2.1. Kinematics of the robot

In order to find out the position and velocity of the end effector or feet of the quadruped robot, the kinematic analysis is very much important. The forward kinematics is essential for a serial-chain manipulator to find out the orientation and position of the end effector in cartesian space with the help of all joint angles and link parameters. With the use of all joint angles, forward kinematics gives only one exact solution. The inverse kinematics is the process of figure out the joint space angles with the help of the position and orientation of the end effector. In this paper, the mechanical model of the quadrupedal robot is divided into two main parts: legs and body or frame.

In the model, each leg has three joints and is actuated by an electric servo motor. It is starting with the assumption that each connection between two links has a single Degree of Freedom (DOF).

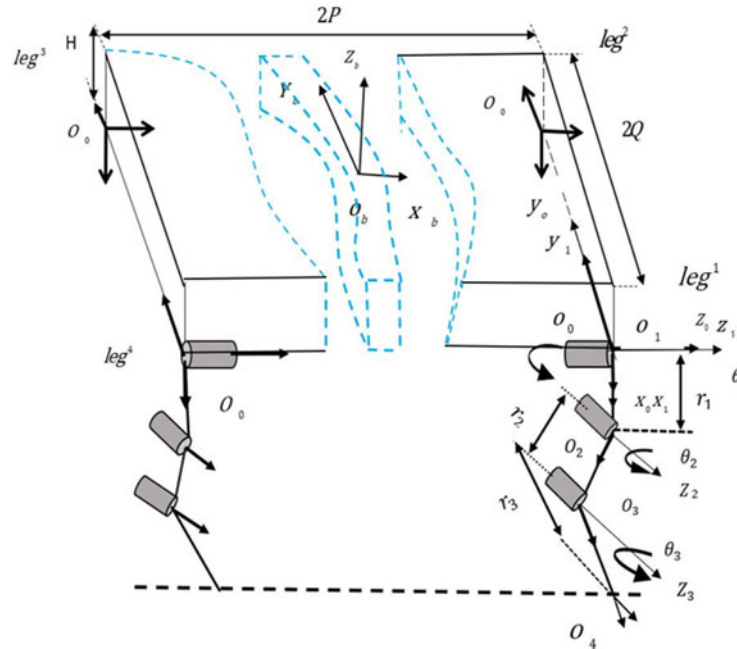


Fig. 2. Skeleton model of quadruped robot.

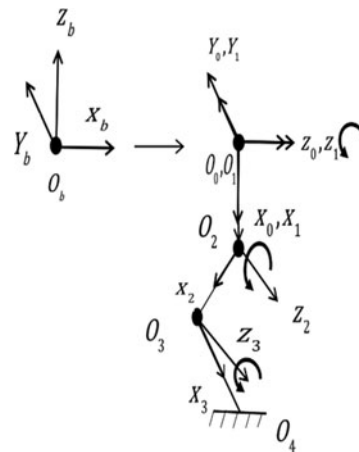


Fig. 3. Coordinate frame of quadruped robot.

A robot leg with n joints means it has $n+1$ links and associates with a joint variable. Each leg of the robot has behaved like a serial manipulator rigidly attached to the coordinate frame to each link. To get the coordinate of the origin of the feet/end effector relative to the base frame by choosing the base frame's origin at any arbitrary point. The origin of the body frame (o_b) is fixed at the geometric center of the torso, and details of the coordinate system for each linkage is shown in Figs. 2–3. The robot forward movement is considered as on the direction x_b and z_b coordinates against the gravity direction. Similarly, the four translational coordinates frames (O_{i_o}) are fixed at each joint of $(leg^l)_{l=1,2,3,4}$ with the torso frame, respectively. The detailed CAD model of the quadruped is shown in Fig. 4.

2.2. D-H parameters

In 1955, Denavit and Hartenberg¹⁵ proposed Denavit-Hartenberg (D-H) transformation matrix for attaching an arbitrary frame to each link of a spatial linkage. The four parameters link twist (α_i),

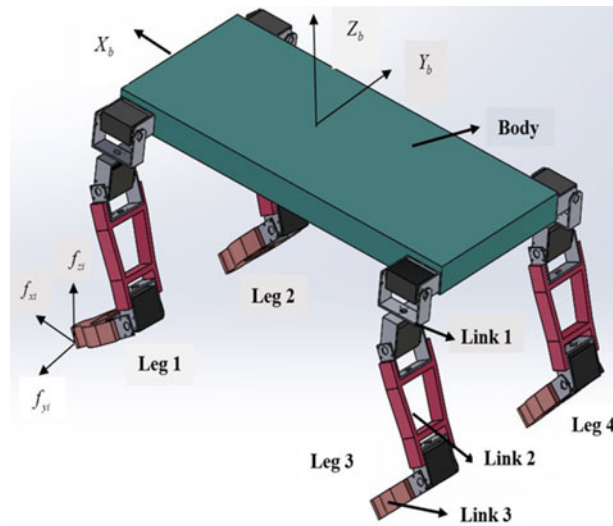


Fig. 4. Four-legged walking robot model.

link length (r_i), joint angle (θ_i), and link offset (d_i) are associated with link (i) and joint (i) in D-H convention method. The coordinate transformation of each link (i) from previous coordinate system ($i-1$) can be obtained in Eq. (1).

$${}^{i-1}T_i = Rot_x(\alpha_{i-1}).Trans_x(r_{i-1}).Rot_z(\theta_i).Trans_z(d_i)$$

$$= \begin{pmatrix} c\theta_i & -s\theta_i & 0 & r_{i-1} \\ s\theta_i c\alpha_{i-1} & c\theta_i c\alpha_{i-1} & -s\alpha_{i-1} & -s\alpha_{i-1}d_i \\ s\theta_i s\alpha_{i-1} & c\theta_i s\alpha_{i-1} & c\alpha_{i-1} & -c\alpha_{i-1}d_i \\ 0 & 0 & 0 & 1 \end{pmatrix} \quad (1)$$

The above equation can be reframed in the form of orientation and position of the end effector in Eq. (2).

$${}^{i-1}T_i = \begin{pmatrix} c\theta_i & -s\theta_i & 0 & r_{i-1} \\ s\theta_i c\alpha_{i-1} & c\theta_i c\alpha_{i-1} & -s\alpha_{i-1} & -s\alpha_{i-1}d_i \\ s\theta_i s\alpha_{i-1} & c\theta_i s\alpha_{i-1} & c\alpha_{i-1} & -c\alpha_{i-1}d_i \\ 0 & 0 & 0 & 1 \end{pmatrix} = \begin{pmatrix} R_{3 \times 3} & P_{3 \times 1} \\ 0 & 1 \end{pmatrix} \quad (2)$$

where $R_{3 \times 3} = \begin{pmatrix} c\theta_i & -s\theta_i & 0 \\ s\theta_i c\alpha_{i-1} & c\theta_i c\alpha_{i-1} & -s\alpha_{i-1} \\ s\theta_i s\alpha_{i-1} & c\theta_i s\alpha_{i-1} & c\alpha_{i-1} \end{pmatrix}$, $P_{3 \times 1} = \begin{pmatrix} r_{i-1} \\ -s\alpha_{i-1}d_i \\ -c\alpha_{i-1}d_i \end{pmatrix}$

Here, $R_{3 \times 3}$ and $p_{3 \times 1}$ are represented as orientation and position of the tip of the feet. Rot_x and Rot_z presents the rotation, $Trans_x$, $Trans_z$ denotes the translation, and $s\theta_i$, $c\theta_i$ are the shortest form of $\sin \theta_i$ and $\cos \theta_i$, respectively. The desired model of Denavit–Hartenberg leg parameters for forward kinematics are given in detail in Fig. 5 and Table I. For a single leg, each transformation matrices of a link from a previous coordinate system can be represented in notations like bT_0 , 0T_1 , 1T_2 , 2T_3 , and 3T_4 . The transformation from the joint (O_{i0}) to coordinate the base frame (O_b) for each leg can be denoted by the constant translational transformation matrix with considering (\pm) sign of σ and ε in Eq. (3).

$${}^bT_0 = \begin{pmatrix} 0 & 0 & 1 & \sigma P \\ 0 & 1 & 0 & \varepsilon Q \\ -1 & 0 & 0 & -H \\ 0 & 0 & 0 & 1 \end{pmatrix} \quad (3)$$

Table I. D-H parameters.

Link	r_{i-1} Link length	α_{i-1} Twist angle	d_i Offset distance	θ_i Joint angle
1	0	0	0	θ_1
2	r_1	90°	0	θ_2
3	r_2	0	0	θ_3
4	r_3	0	0	0

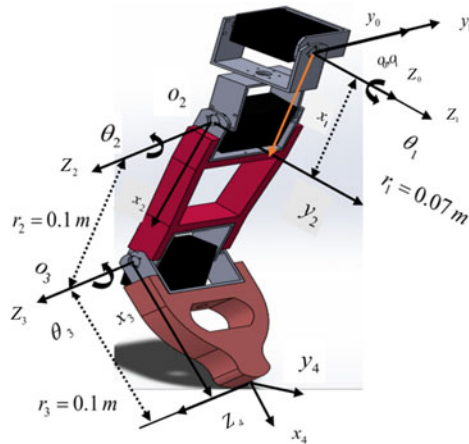


Fig. 5. D-H parameters of a leg frame.

where P , Q , and H are represented as structural parameters of the robot frame. The deduction of a homogeneous transformation matrix nearby coordinate systems is as follows (4)–(8):

$${}^bT_0 = \text{Trans}(P, Q, -H)\text{Rot}(y, 90^0) \tag{4}$$

$${}^0T_1 = \text{Rot}(z, \theta_1) \tag{5}$$

$${}^1T_2 = \text{Rot}(x, 90^\circ)\text{Tran}(r_1, 0, 0)\text{Rot}(z, \theta_2) \tag{6}$$

$${}^2T_3 = \text{Tran}(r_2, 0, 0)\text{Rot}(z, \theta_3) \tag{7}$$

$${}^3T_4 = \text{Tran}(r_3, 0, 0) \tag{8}$$

Similarly, the coordinate of four feet in the base frame can be obtained by multiplying bT_0 with 0T_4 the transformation matrix. The position coordinates of one foot of $\text{leg}^l_{l=1}$ with respect to the base frame are given in detail from Eqs. (9) to (11).

$$p_x = r_2s\theta_2 + r_3s\theta_{23} + P \tag{9}$$

$$p_y = r_1s\theta_1 + r_2s\theta_1c\theta_2 + r_3s\theta_1c\theta_{23} - Q \tag{10}$$

$$p_z = r_1c\theta_1 - r_2c\theta_1c\theta_2 - r_3c\theta_1c\theta_{23} - H \tag{11}$$

where $c\theta_{23} = \cos(\theta_2 + \theta_3) = \cos\theta_2\cos\theta_3 - \sin\theta_2\sin\theta_3$, $s\theta_{23} = \sin(\theta_2 + \theta_3) = \sin\theta_2\cos\theta_3 + \cos\theta_2\sin\theta_3$ and p_x , p_y , and p_z are denoted as the elements of the position vector.

2.3. Inverse kinematic

The inverse kinematic solution is needed for motion planning and control of manipulators to achieve the required movement. For that, it is necessary to convert position and rotational of manipulator end effectors from Cartesian space to joint space. Due to each leg’s identical posture, one leg joint variables’ value is to be calculated from the inverse kinematics equation and remained the same for other legs. In this paper, we calculate in detail the joint variables by the inverse kinematic equation

of $leg^l)_{l=1}$ by the use of end effectors coordinates (p_x, p_y, p_z) in base global point (O_b) . The three joint variables are given directly as follows in Eqs. (12)–(14):

$$\theta_1 = \tan^{-1} - \left(\frac{Q + p_z}{H + p_z} \right) \tag{12}$$

$$\theta_2 = \cos^{-1} \left(\frac{M^2 + N^2 - r_2^2 - r_3^2}{2r_2r_3} \right) \tag{13}$$

where $M = (-r_1 + p_y s\theta_1 - Hc\theta_1 + Qs\theta_1 - p_z c\theta_1)$, $N = (p_x - P)$

$$\theta_3 = a \tan 2(N, M) \pm a \tan 2(\sqrt{(N^2 + M^2 - K^2)}, K), \quad \text{where } K = r_2 + r_3 c\theta_3 \tag{14}$$

2.4. Dynamic modeling of four-legged robot

Multi-legged robots are very complex, and composite mechanics set up. Each leg of a quadruped robot is tied up to one another through the body frame and finally making a closed kinematic chain through the ground. Forces and moments are acting on a robot mechanism transmit through the kinematic chain from one link to another. The equation of motion for a robot control system with four legs (each leg with three DOF) is deduced by using Lagrangian dynamics formulation, and the general equation of the i th n -DOF leg can be represented in vector-matrix form, as shown in Eq. (15).

$$\tau_i - \tau_{if} - J_{gi}^T F_{gi} + J_{ei}^T F_{ei} = [H(\theta)]_i [\ddot{\theta}]_i + C_i(\theta_i, \dot{\theta}_i)\dot{\theta}_i + [\tau_g(\theta)]_i \tag{15}$$

In this equation $\theta, \dot{\theta}, \ddot{\theta}$ and τ are vector of joint position, velocity, acceleration, and force variables, respectively. Where $H(\theta)^{3 \times 3}$ is mass inertia matrix of the leg, $\theta_i^{3 \times 1}$ is joint position vector, $C_i(\theta_i, \dot{\theta}_i)^{3 \times 1}$ is a vector of centrifugal/Coriolis terms, $\tau_{gi}(\theta_i)^{3 \times 1}$ is a of gravitational forces/torques terms, $\tau_i^{3 \times 1}$ is the vector of joint torques. F_{ei} and F_{gi} are the 3×1 vector of coupled force of legs with body and ground forces, respectively. In the leg’s air swing stage, the ground reaction force becomes zero, as there is no interaction between foot and ground. But in the stance phase case, ground reaction force plays an important role due to foot and ground interaction.

2.5. Torso body dynamics

Defining $x_b \in \mathbb{R}^n$ as the position coordinates vector of the torso frame, the dynamics of the quadrupedal robot body is expressed as follows in Eq. (16):

$$F_b = H_b(x_b)\ddot{x}_b + C_b(x_b, \dot{x}_b)\dot{x}_b + G_b(x_b) \tag{16}$$

where $F_b \in \mathbb{R}^n$ denotes the command forces or spatial force in the operational space acting on the center of mass of the torso body, $H_b(x_b) \in \mathbb{R}^{n \times n}$ is the positive symmetric definite inertia matrix, $C_b(x_b, \dot{x}_b) \in \mathbb{R}^{n \times n}$ is the Coriolis/centrifugal matrix, and $G_b(x_b) \in \mathbb{R}^{n \times 1}$ is the $(n \times 1)$ vector gravity force.

Let us define the Jacobian matrix $J(\theta) \in \mathbb{R}^{n \times n}$ transfers the joint velocity $(\theta \in \mathbb{R}^n)$ to the spatial vector acting on the trunk of body velocity $(x_b \in \mathbb{R}^n)$ according to

$$x_b = J(\theta)\dot{\theta}$$

The final dynamic expression can be denoted as in Eq. (17)²⁵

$$H\ddot{\theta} + C\dot{\theta} + G = \tau - \tau_f - J_g^T F_g \tag{17}$$

2.6. Calculation of feet forces

The distribution of the body force of the feet is the major task for a robot dynamic. The underlying assumptions are considered for computing feet forces distribution:

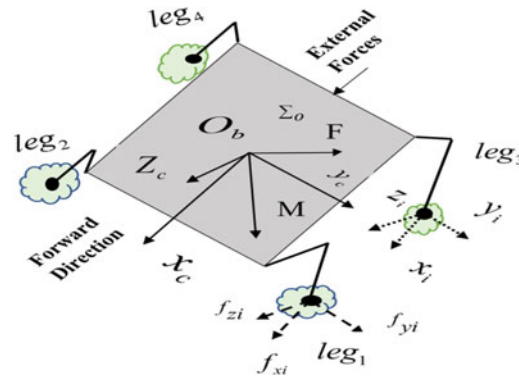


Fig. 6. Forces acting on a quadruped robot.

Assumption 1. It is assumed that legs are carried and the load considering no slippage between the tip of feet and the terrain contact point.

Assumption 2. The reciprocal action between tips of the leg and ground surface must be point contact with friction, which means that legs exert on the supporting surface through the foot are limited to three components of forces: one perpendicular and the other two horizontal to the surfaces.

Assumption 3. During leg movements, it is assumed that the center of gravity of the robot does not shift significantly, and the effect of the inertia of transfer legs on the robot body is equivalent to zero.

Approach 1. Foot Forces Calculation.

There are only two possible support-phases: three-leg grounded phase and four-leg grounded phase to analyze the feet force for the statistically stable walk. The different force acting on a four-footed robot is shown in Fig. 6. Now consider that $F = [f_{ix}, f_{iy}, f_{iz}]$ is the ground reaction force vector passes upward from the foot i , where $i = 1, 2, 3...q$, q is the number of legs supported in the ground for a particular instant. The wrench $W = [F_{ix}, F_{iy}, F_{iz}, M_x, M_y, M_z]^T$ contains the forces and moments acting on the robot’s center of gravity (C.G), considering the effect of a surface gradient, weight, and inertia of the moving segment of robot’s body. Then without considering the inertia effect of the transfer legs, six equilibrium equations of balance forces and moments can be written in Eqs. (18)–(23) as follows:

$$F_x + \sum_{i=1}^q f_{ix} = 0 \tag{18}$$

$$F_y + \sum_{i=1}^q f_{iy} = 0 \tag{19}$$

$$F_z + \sum_{i=1}^q f_{iz} = 0 \tag{20}$$

$$\sum_{i=1}^n y_i f_{iz} - \sum_{i=1}^n z_i f_{iy} + y_c F_z - z_c F_y + M_x = 0 \tag{21}$$

$$\sum_{i=1}^n z_i f_{ix} - \sum_{i=1}^n x_i f_{iz} + z_c F_x - x_c F_z + M_y = 0 \tag{22}$$

$$\sum_{i=1}^n x_i f_{iy} - \sum_{i=1}^n y_i f_{ix} + x_c F_y - y_c F_x + M_z = 0 \tag{23}$$

Under these conditions, six equilibrium equations that balance forces and moments can be written in matrix form as given below.

$$\begin{bmatrix} 1 & 0 & 0 & 1 & 0 & 0 & 1 & 0 & 0 \\ 0 & 1 & 0 & 0 & 1 & 0 & 0 & 1 & 0 \\ 0 & 0 & 1 & 0 & 0 & 1 & 1 & 0 & 1 \\ 0 & -z_1 & y_1 & 0 & -z_2 & y_2 & 0 & -z_3 & y_3 \\ z_1 & 0 & -x_1 & z_2 & 0 & -x_2 & z_3 & 0 & -x_3 \\ -y_1 & x_1 & 0 & -y_2 & x_2 & 0 & -y_3 & x_3 & 0 \end{bmatrix}_{6 \times 9} \begin{bmatrix} f_{1x} \\ f_{1y} \\ f_{1z} \\ f_{2x} \\ f_{2y} \\ f_{2z} \\ f_{3x} \\ f_{3y} \\ f_{3z} \end{bmatrix}_{9 \times 1} = \begin{bmatrix} F_x \\ F_y \\ F_z \\ M_x \\ M_y \\ M_z \end{bmatrix}_{6 \times 1} \tag{24}$$

where $[x_i, y_i, z_i]$ are the coordinates of i th foot-ground contact point with respect to body reference frame (o_b) and $[x_c, y_c, z_c]$ are the position of $C.G$ of the robot with respect to body reference frame.

The Eq. (24) can be rearranged in matrix form as shown in Eq. (25).

$$[P][F] = -[N][W] \tag{25}$$

where, $P_1 = \begin{bmatrix} I_3 & I_3 & I_3 \\ S_A & S_B & S_C \end{bmatrix}_{6 \times 9}$ and $[F] = [F_A \ F_B \ F_C]$ for $\beta = 1/2$

$P_2 = \begin{bmatrix} I_3 & I_3 & I_3 & I_3 \\ S_A & S_B & S_C & S_D \end{bmatrix}_{6 \times 12}$ and $[F] = [F_A \ F_B \ F_C \ F_D]$ for $\beta = 2/3$

The tip of foot i ($i = A, B, C$ for three-leg support; where $\beta = 1/2$). During the three-leg support phase, P becomes P_1 and dimensions of the matrix 6×9 , whereas the remaining phases, P becomes P_2 with the size of the matrix 6×12 .

where $N = \begin{bmatrix} I_3 & 0_3 \\ S_c & I_3 \end{bmatrix}$, $S_i = \begin{bmatrix} 0 & -z_i & y_i \\ z_i & 0 & -x_i \\ -y_i & x_i & 0 \end{bmatrix}$

I_3 is the identity matrix with size (3×3) , 0_3 is the null matrix with dimension (3×3) , and S_i is a skew-symmetric matrix. By considering the feet-tip position, the feet forces during the entire leg motion can be calculated using the least-square method.²³ The solution of Eq. (25) is indeterminate, as it has six equations involving nine variables. The least-square method can be used to get the minimum solution of the indeterminate equilibrium equation. The solution is written in matrix form in Eq. (26).

$$F = -P^T [(P)[P]^T]^{-1} ([N][W]) \tag{26}$$

In the above equation, pseudoinverse can also be obtained by multiplying the transpose matrix from the right, and this is called a generalized right inverse: $P_{right}^{-1} = P^T [(P)[P]^T]^{-1}$.²⁶⁻²⁷ Where, P having a full rank, $[P.P^T]$ is a positive definite matrix.

Approach 2. Joint Torque Calculation.

In this approach, joints torque can be calculated with Eq. (25) using the following relation:

$$F = [K][\tau], \text{ where } [K] = \begin{bmatrix} A_J & 0_J & 0_J \\ 0_J & B_J & 0_J \\ 0_J & 0_J & C_J \end{bmatrix}_{9 \times 9}$$

$[K]$ will have the dimension (9×9) (for three-leg support). $[\tau] = [\tau_A \tau_B \tau_C]^T$ and $\tau_i = [\tau_{i1} \tau_{i2} \tau_{i3}]^T$ is the torque vector consisting of joint torques at leg i , respectively.

The Eq. (25) can be written as

$$P_j [K] [\tau] = - [N] \cdot [W] \quad (27)$$

$$P_j [\tau] = - [N] \cdot [W] \quad (28)$$

Again, the least-square method can be used to find the exact solution of the above indeterminate equation.²⁸ The final equation can be rearranged in matrix form as expressed in Eq. (29).

$$[\tau] = -P_j^T [(P_j)[P_j]^T]^{-1} ([N][W]) \quad (29)$$

The feet forces can be obtained using the help of Eq. (25).

3. Power Consumption

To perform any task in a quadruped robot is only possible due to energy utilized by the motors tied to the joints of the legs. In a multi-legged robot, minimizing energy consumption with different environmental conditions are the most challenging problem.^{29,30} In a particular environmental condition, the value of the joint velocity and torque leads to the energy utilization of each joint and then the total system. The total energy can be expressed as

$$E = E_m + E_e \quad (30)$$

where E_m stands for mechanical energy and E_e indicates heat energy loss. Furthermore, the above equation can be expanded with energy utilized by each motor of joint (i) of the leg (l) during a time period (t) as written in Eq. (31).^{31,32}

$$E_{Total} = \int_0^t V_a I_a dt = \int_0^t \sum_{leg(l=1)}^n \sum_{i=1}^n \delta(\tau_i \dot{\theta}_i) dt + \int_0^t \sum_{leg(l=1)}^n \sum_{i=1}^n R_i \left(\frac{\tau_i}{G_i K_i} \right)^2 dt \quad (31)$$

where

$$\delta(\tau \dot{\theta}) = \begin{cases} \tau \dot{\theta}, & \text{if } \tau \dot{\theta} \text{ greater than '0'} \\ 0, & \text{if } \tau \dot{\theta} \text{ less than equal to '0'} \end{cases}$$

V_a and I_a are the input voltage and current, respectively. Here, τ represent as joint torque and $\dot{\theta}$ indicates the rotational velocity. Where R_i , G_i , and K_i are the armature resistance, gear ratio, and torque constant, respectively. Now, the total energy utilized by 12 motors of a quadruped robot can be found out in Eq. (32).

$$E_{Total} = \int_0^t V_a I_a dt = \int_0^t \sum_{leg(l=1)}^4 \sum_{i=1}^3 \delta(\tau_i \dot{\theta}_i) dt + \int_0^t \sum_{leg(l=1)}^4 \sum_{i=1}^3 R_i \left(\frac{\tau_i}{G_i K_i} \right)^2 dt \quad (32)$$

The average power is the time average of the instantaneous power or total power. Then, average power utilization can be determined as follows:

$$\text{Average Power } P_{ave} = E_{Total}/T \quad (33)$$

4. Numerical Result Analysis

The primary mechanism of a legged robot must generate enough force to support its own weight and as well as move the body. The fundamental distinction between walking and running gait is that walking gait has a duty factor of more than 0.5 whereas running gait less than 0.5. In walk gait, both the pair of feet are on the ground simultaneously, but in running gait, both the pair of feet are off the ground. In asymmetrical gait, each pair of the leg has the same duty factor and with a 0.5 phase difference. Before investigating the quadruped robot's leg characteristics, we considered specific input parameters such as the physical dimensions, moving velocity, stride length, and duty

Table II. Physical parameters of each link.

Link descriptions	Unit	Symbol	Link ¹	Link ²	Link ³
Length	mm	r	65	100	100
Mass	kg	m	0.033	0.04	0.05
Center of mass	mm	x_{cm}	144.9	67.9	149
		y_{cm}	-72.7	-15.33	-23.8
		z_{cm}	-24.42	40	-23.8
Moment of inertia	$\text{g}\cdot\text{mm}^2$	I_{xx}	227,510.9	124,348.8	94,685.9
		I_{yy}	775,870.1	287,769.6	1,302,407.5
		I_{zz}	951,175.5	274,075.58	13,302,288.9
Product of inertia	$\text{g}\cdot\text{mm}^2$	I_{xy}	-374,154	-43,324.76	-198,167.3
		I_{xz}	-126,675	114,921.2	-198,343.9
		I_{zy}	62,894.1	-25,939.7	31,530.5
Body parameters					
Product of inertia (body)	$\text{kg}\cdot\text{m}^2$	I_{xx}	0.30		
		I_{yy}	0.05		
		I_{zz}	0.32		
Weight of the body	kg	m	1.30		

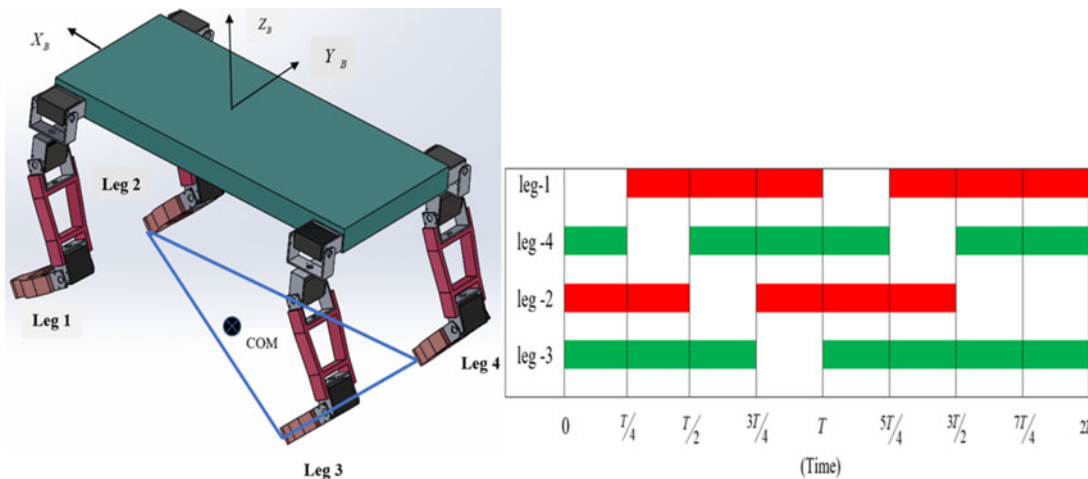


Fig. 7. Walking gait pattern with support polygon of duty factor 0.75.

cycle. The detail of the simulation parameters of each leg of the quadruped robot is show in Table II. The Jacobian matrix of the leg “ l ” can be written as

$$j_l = \begin{bmatrix} \frac{\partial x_l}{\partial \theta_1} & \frac{\partial x_l}{\partial \theta_2} & \frac{\partial x_l}{\partial \theta_3} \\ \frac{\partial y_l}{\partial \theta_1} & \frac{\partial y_l}{\partial \theta_2} & \frac{\partial y_l}{\partial \theta_3} \\ \frac{\partial z_l}{\partial \theta_1} & \frac{\partial z_l}{\partial \theta_2} & \frac{\partial z_l}{\partial \theta_3} \end{bmatrix}$$

Here, it is assumed that the quadruped robot moving in the x -direction with the leg sequence generated 4-3-2-1, as shown in Fig. 7. Body height and velocity are considered to be equal to 0.1 m and 0.05 m/s, respectively. The stride length and cycle time are measured to be equal to 0.1 m and 0.4 s, respectively. Duty factor (percent of the foot on the ground on cycle time), $\beta = 0.75$.

Table III. Average power utilization obtained by two approaches.

Approaches	Average value (watts)
Approach 1	0.0672
Approach 2	0.1152

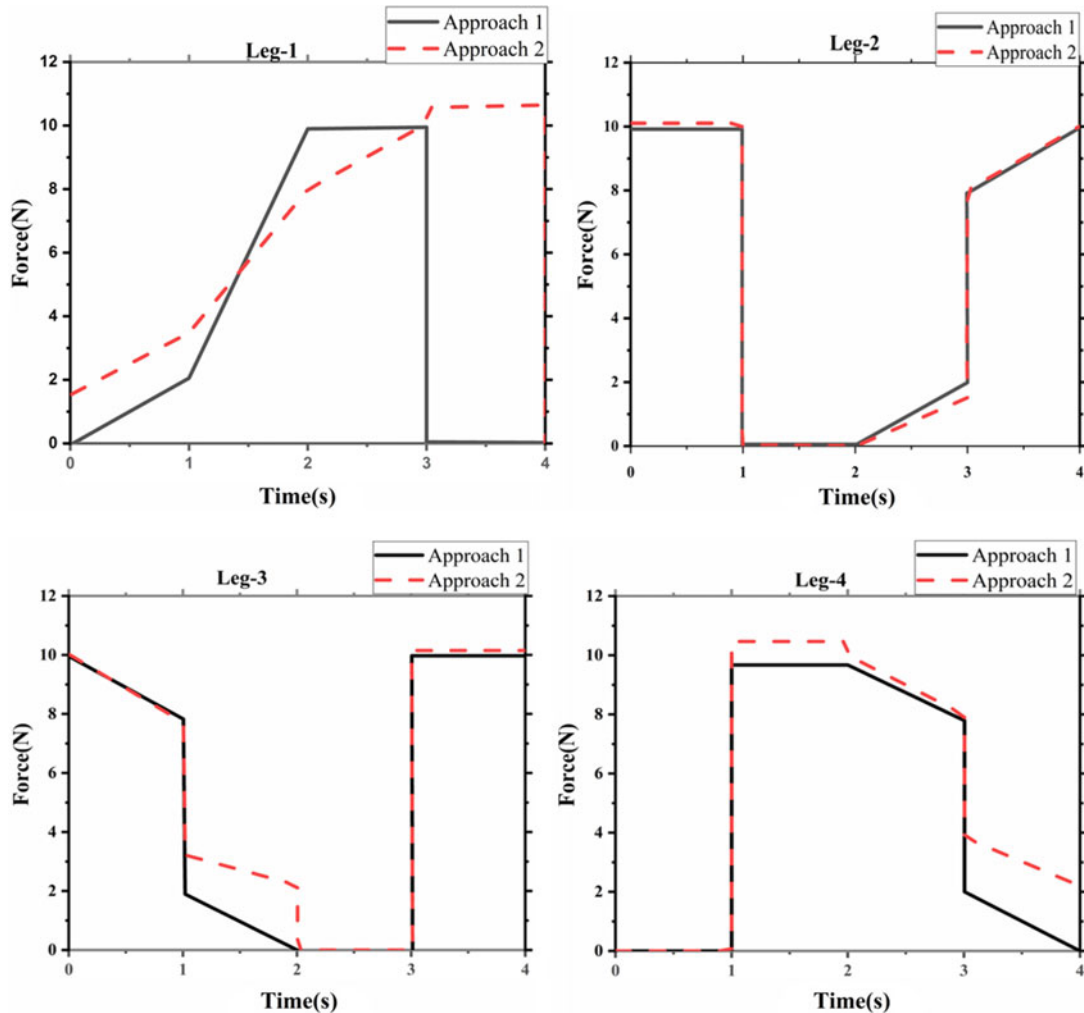


Fig. 8. Feet force distribution by approaches 1 and 2.

The distribution of foot forces is shown in Fig. 8, which is obtained by approaches 1 and 2. The cycle time of one locomotion is set as 0–4 s. In Fig. 8, it is observed that the front and hind legs are complemented each other in force. The total weight of the robot is the sum of all the vertical force of each ground contact legs for a particular time. In Approach 1, it is observed that the horizontal component tends to zero during robot uniform motion, which signifies that the friction does not influence the total system. In the second approach, horizontal direction forces are observed to predominate in which the findings are almost close to that published by Eden and Leblehiciolu.³³

The variation of torques at each joint is shown in Figs. 9–10, obtained by approaches 1–2. It is observed that joint 2 produced more torque compared to another joint during the locomotion. In Approach 1, the torque variation is more (basically joint 2) than other joints of legs. However, it seems to be less variation of torques of a different joint of the motor in Approach 2. The motor (joint 2) can be selected over the underutilized at joints 1 and 3 based on Approach 2.

In Table III, the average values of a robot's joint power consumption can be obtained by two approaches using Eq. (33). Figures 9 and 10 show that the average torque of Approach 1 is less

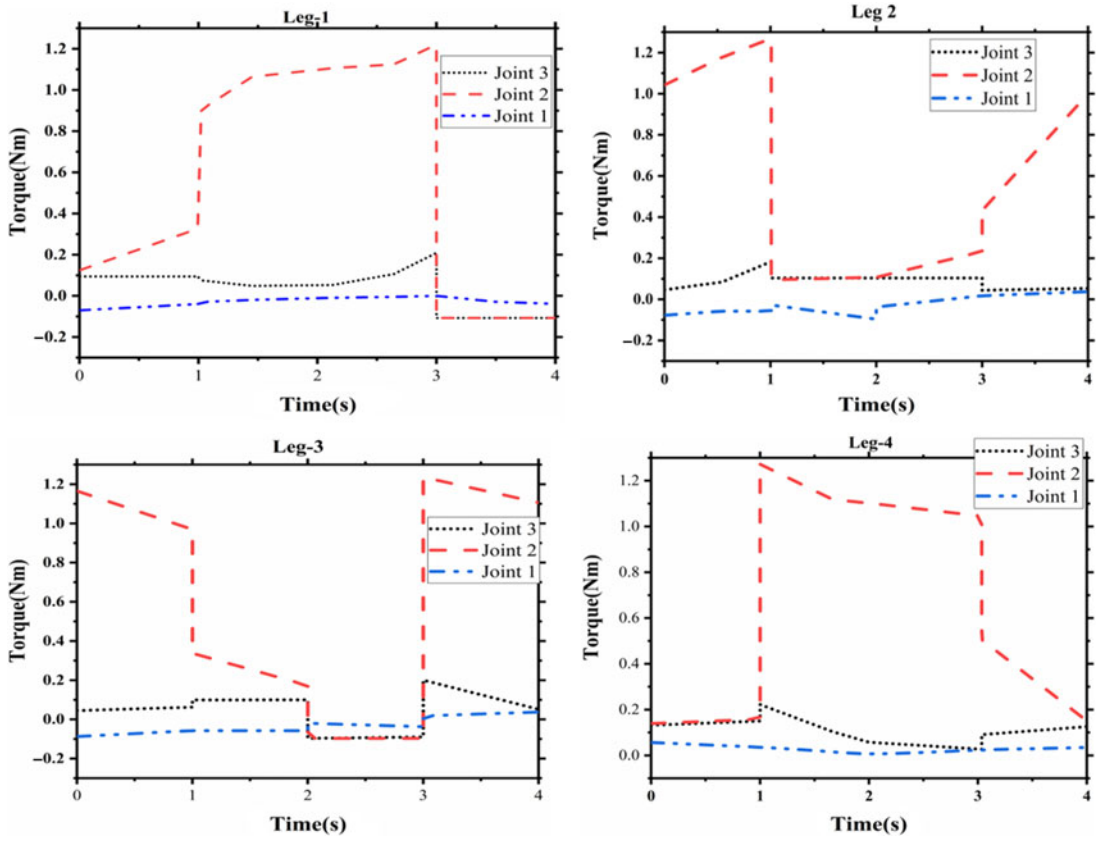


Fig. 9. Torque at each actuator of the legs by Approach 1.

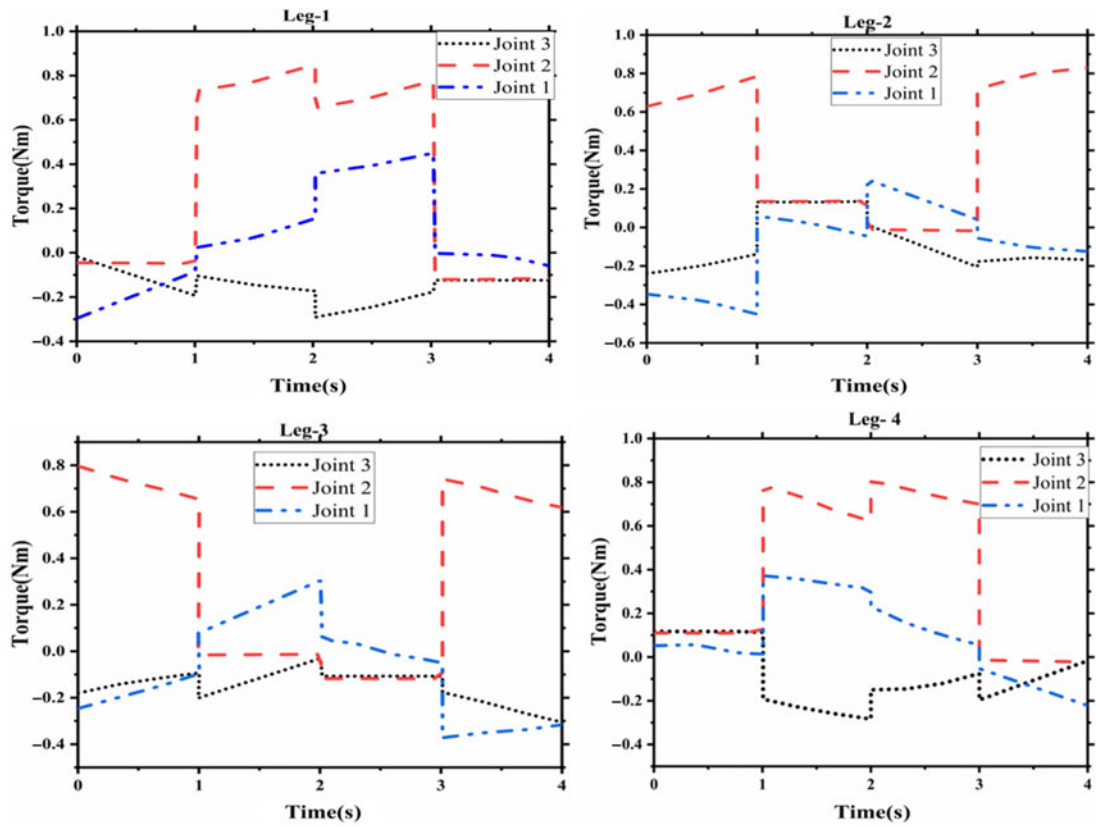


Fig. 10. Torque at each actuator of the legs by Approach 2.

compared to Approach 2. As power utilization of the motor or system is directly proportional to torque, Approach 1 is more power-efficient than Approach 2.

5. Conclusions

In this paper, both the kinematics and dynamics of a quadruped robot's mathematical model have been developed. A single-leg kinematic model has been developed using forward and inverse kinematics to achieve statically stable gait.

1. By considering an external wrench, the distribution of required forces and moments on a quadruped robot's supporting legs is operated as feet force distribution.
2. Two approaches have been modeled to get the optimal distribution of feet forces. The first approach has provided more energy-efficient and more joint torques variation in comparison to Approach 2.
3. The Euler–Lagrangian formulation is used to calculate the joint torque of each joint. It is also observed that the supporting phase joint torques are more than the transfer phase leg.
4. The proposed kinematic and dynamics have been tested for the walking gait of a developed quadruped robot. In the future, work can be incorporated into a multi-legged robot to tackle the drawback related to discontinuous and non-synchronized gait.

Acknowledgments

The authors would like to acknowledge the support from the Science & Engineering Research Board (SERB), a statutory body of the Department of Science & Technology, (DST) Government of India.

References

1. X. Meng, S. Wang, Z. Cao and L. Zhang, "A Review of Quadruped Robots and Environment Perception," *2016 35th Chinese Control Conference (CCC), IEEE* (2016) pp. 6350–6356.
2. H. Zhuang, H. Gao, Z. Deng, L. Ding and Z. Liu, "A review of heavy-duty legged robots," *Sci. China Tech. Sci.* **57**(2), 298–314 (2014).
3. Y. Zhong, R. Wang, H. Feng and Y. Chen, "Analysis and research of quadruped robot's legs: A comprehensive review," *Int. J. Adv. Robot. Syst.* **16**(3), 1729881419844148 (2019),
4. D. C. Kar, "Design of statically stable walking robot: A review," *J. Robot. Syst.* **20**(11), 671–686 (2003).
5. F. Rubio, F. Valero and C. Llopis-Albert, "A review of mobile robots: Concepts, methods, theoretical framework, and applications," *Int. J. Adv. Robot. Syst.* **16**(2), 1729881419839596 (2019).
6. D. J. Todd, *Walking Machines: An Introduction to Legged Robots* (Springer Science & Business Media, Springer US, 2013).
7. X. Ding and H. Chen, "Dynamic modeling and locomotion control for quadruped robots based on center of inertia on SE (3)," *J. Dyn. Syst. Meas. Control* **138**(1), 011004 (2016) Paper No: DS-15-1298. doi: [10.1115/1.4031728](https://doi.org/10.1115/1.4031728).
8. C. Gehring, S. Coros, M. Hutter, M. Bloesch, M. A. Hoepflinger and R. Siegwart, "Control of Dynamic Gaits for a Quadrupedal Robot," *2013 IEEE International Conference on Robotics and Automation (IEEE, 2013)* pp. 3287–3292.
9. J. Zhang, F. Gao, X. Han, X. Chen and X. Han, "Trot gait design and CPG method for a quadruped robot," *J. Bionic Eng.* **11**(1), 18–25 (2014).
10. B. S. Lin and S. M. Song, "Dynamic modeling, stability, and energy efficiency of aquadrupedal walking machine," *J. Robot. Syst.* **18**(11), 657–670 (2001).
11. A. Mahapatra, S. S. Roy and D. K. Pratihar, "Study on feet forces' distributions, energy consumption and dynamic stability measure of hexapod robot during crab walking," *Appl. Math. Model.* **65**, 717–744 (2019). doi: [10.1016/j.apm.2018.09.015](https://doi.org/10.1016/j.apm.2018.09.015).
12. M. Liu, D. Qu, F. Xu, F. Zou, P. Di and C. Tang, "Quadrupedal robots whole-body motion control based on centroidal momentum dynamics," *Appl. Sci.* **9**(7), 1335 (2019).
13. Z. Li, S. S. Ge and S. Liu, "Contact-force distribution optimization and control for quadruped robots using both gradient and adaptive neural networks," *IEEE Trans. Neural Netw. Learn. Syst.* **25**(8), 1460–1473 (2013).
14. W. L. Ma, K. A. Hamed and A. D. Ames, "First steps towards full model-based motion planning and control of quadrupeds: A hybrid zero dynamics approach," arXiv preprint [arXiv:1909.08124](https://arxiv.org/abs/1909.08124) (2019).
15. D. Howard, S. J. Zhang and D. J. Sanger, "Kinematic analysis of a walking machine," *Math. Comput. Simul.* **41**(5–6), 525–538 (1996).
16. D. M. Gorinevsky and A. Y. Shneider, "Force control in locomotion of legged vehicles over rigid and soft surfaces," *Int. J. Robot. Res.* **9**(2), 4–23 (1990).
17. J. P. Barreto, A. Trigo, P. Menezes, J. Dias and A. T. De Almeida, "FED-the Free Body Diagram Method. Kinematic and Dynamic Modeling of a Six-Leg Robot," *AMC'98-Coimbra. 1998 5th International Workshop on Advanced Motion Control. Proceedings (Cat. No. 98TH8354)* (IEEE, 1998) pp. 423–428.

18. Z. Li, S. S. Ge and S. Liu, "Contact-force distribution optimization and control for quadruped robots using both gradient and adaptive neural networks," *IEEE Trans. Neural Netw. Learn. Syst.* **25**(8), 1460–1473 (2013).
19. X. Chen, K. Watanabe, K. Kiguchi and K. Izumi, "Optimal force distribution for the legs of a quadruped robot," *Mach. Intell. Robot. Control* **1**(2), 87–93 (1999).
20. D. Zhou, K. H. Low and T. Zielinska, "An efficient foot-force distribution algorithm for quadruped walking robots," *Robotica* **18**(4), 403–413 (2000).
21. W. Y. Jiang, A. M. Liu and D. Howard, "Foot-Force Distribution in Legged Robots," *Proceedings of Fourth International Conference on Climbing and Walking Robots, Karlsruhe, Germany* (2001) pp. 331–338.
22. D. W. Marhefka and D. E. Orin, "Quadratic Optimization of Force Distribution in Walking Machines," *Proceedings. 1998 IEEE International Conference on Robotics and Automation (Cat. No. 98CH36146)*, vol.1 (1998) pp. 477–483.
23. Y. Zheng, C. M. Chew and A. H. Adiwahono, "A GJK-based approach to contact force feasibility and distribution for multi-contact robots," *Robot. Auto. Syst.* **59**(3–4), 194–207 (2011).
24. D. C. Kar, K. KurienIssac and K. Jayarajan, "Minimum energy force distribution for a walking robot," *J. Robot. Syst.* **18**(2), 47–54 (2001).
25. S. S. Roy and D. K. Pratihar, "Effects of turning gait parameters on energy consumption and stability of a six-legged walking robot," *Robot. Auto. Syst.* **60**(1), 72–82 (2012).
26. L. Tan, *A Generalized Framework of Linear Multivariable Control* (Butterworth-Heinemann, Newton, MA, 2017).
27. S. R. Buss, "Introduction to inverse kinematics with jacobian transpose, pseudoinverse and damped least squares methods," *IEEE J. Robot. Autom.* **17**(1–19), 16 (2004).
28. J. D. Hoffman and S. Frankel, *Numerical Methods for Engineers and Scientists* (CRC Press, Boca Raton, FL, 2018).
29. J. Rigelsford, "Robotics: Control, sensing, vision and intelligence," *Ind. Robot Int. J.* **26**(2) (1999). doi:[10.1108/ir.1999.04926bae.002](https://doi.org/10.1108/ir.1999.04926bae.002).
30. B. Jin, C. Chen and W. Li, "Power consumption optimization for a hexapod walking robot," *J. Intell. Robot. Syst.* **71**(2), 195–209 (2013).
31. Z. Hua, X. Rong, Y. Li, H. Chai, B. Li and S. Zhang, "Analysis and verification on energy consumption of the quadruped robot with passive compliant hydraulic servo actuator," *Appl. Sci.* **10**(1), 340 (2020).
32. K. Yang, X. Rong, L. Zhou and Y. Li, "Modeling and analysis on energy consumption of hydraulic quadruped robot for optimal trot motion control," *Appl. Sci.* **9**(9), 1771 (2019).
33. M. S. Erden and K. Leblebicioglu, "Torque distribution in a six-legged robot," *IEEE Trans. Robot* **23**(1), 179–186 (2007).